Separation Science and Technology
Publication details, including instructions for authors and subscription information:
http://www.informaworld.com/smpp/title~content=t713708471

Resistance Analyses for Ultrafiltration in Tubular Membrane Module

T. W. Cheng[a]; H. M. Yeh[a]; C. T. Gau[a]
[a] DEPARTMENT OF CHEMICAL ENGINEERING, TAMKANG UNIVERSITY, TAIWAN, REPUBLIC OF CHINA

To cite this Article Cheng, T. W. , Yeh, H. M. and Gau, C. T.(1997) 'Resistance Analyses for Ultrafiltration in Tubular Membrane Module', Separation Science and Technology, 32: 16, 2623 — 2640
To link to this Article: DOI: 10.1080/01496399708006960
URL: http://dx.doi.org/10.1080/01496399708006960

SEPARATION SCIENCE AND TECHNOLOGY, 32(16), pp. 2623–2640, 1997

Resistance Analyses for Ultrafiltration in Tubular Membrane Module

T. W. CHENG,* H. M. YEH, and C. T. GAU
DEPARTMENT OF CHEMICAL ENGINEERING
TAMKANG UNIVERSITY
TAMSUI 251, TAIWAN, REPUBLIC OF CHINA

ABSTRACT

The resistance analyses for ultrafiltration of macromolecular solutions by the resistances-in-series model and the modified gel-polarization model, respectively, have been extended to the turbulent ultrafiltration system in this study. The experiments are carried out by ultrafiltrating dextran T500 solutions in a tubular membrane module with membrane material of ZrO_2-TiO_2/carbon. It is found that the permeate fluxes are predicted very well by these models for both laminar and turbulent systems, and the resistance caused by the concentration polarization/gel layer (R_p) can be reduced by increasing the crossflow velocity on the membrane surface. Analysis by the resistances-in-series model showed that, R_p decreases with flow velocity with exponents of 0.49 and 0.99 for the laminar system and the turbulent system, respectively.

Key Words. Ultrafiltration; Resistance in series; Gel polarization; Concentration polarization; Tubular; Fouling

INTRODUCTION

Ultrafiltration of macromolecular solutions has become an increasingly important separation process. The applications of ultrafiltration include the treatment of industrial effluents, oil emulsion wastewater, biological macromolecules, colloidal paint suspensions, medical therapeutics, etc.

* To whom correspondence should be addressed.

The rapid development of this process was made possible by the advent of anisotropic, high-flux membranes capable of distinguishing among molecular and colloidal species in the 0.001 to 10 μm size range.

This process is a pressure-driven membrane separation process. The applied pressure, usually in the 1 to 10 bar range, provides the driving potential to force the solvent to flow through the membrane, and the solute is rejected by the membrane. The concentration of solute on the membrane surface is higher than that in the bulk solution. This is known as concentration polarization. As the solute accumulates on the membrane surface, a membrane fouling phenomena such as solute adsorption occurs.

For a small applied pressure, the solvent flux through the membrane is observed to be proportional to the applied pressure. However, when the pressure is increased further, the flux begins to drop below that which results from a linear flux–pressure behavior. Eventually a limiting flux is reached where any increase in pressure will not lead to a further increase in the permeate flux. Two different models are adopted to elucidate this phenomenon: the gel-polarization model (1–6) and the osmotic-pressure model (7–13). According to the former model, the solute forms a gel layer at the membrane surface, the gel concentration is constant, and the thickness of the gel layer increases with applied pressure (14). The second model regards the limiting flux as a consequence of the increased osmotic pressure produced by the high concentration of the rejected solute near the membrane surface, and the concentration of the rejected solute increases with applied pressure (8).

The permeate flux for ultrafiltration of macromolecular solutions is well described by the resistance-in-series model. It regards the transport resistances to be due to the intrinsic membrane, the concentration polarization/gel layer, and the fouling phenomena. Chiang and Cheryan (15) analyzed the ultrafiltration of skim milk in a hollow-fiber membrane module by this model, but the fouling resistance was not observed to be affected by the operating parameters. Nabetani et al. (16) ultrafiltrated macromolecular solutions in a plate-and-frame membrane module. The experimental data showed that the fouling resistance increases with an increase in the solute concentration. Yeh and Cheng (17) ultrafiltrated dextran T500 solutions in a hollow-fiber membrane module and found the resistances to be functions of such operating parameters as the transmembrane pressure, the feed concentration of the solute, and the flow velocity. Recently, Gomez-Gotor et al. (18) used this model to analyzed the experimental data of starch/water solutions in a plane membrane ultrafiltration module. Based on the concept of the resistance-in-series model, Yeh (19) derived a modified gel-polarization model and successfully correlated the permeate flux

data obtained from previous work (17) in conditions of lower transmembrane pressure.

The previous analyses were confined to experimental data in the laminar flow region. In present work we will investigate the influences of the operating parameters on the transport resistances for ultrafiltration in both laminar and turbulent flow regions. A macromolecular solution will be ultrafiltrated in a tubular membrane module under the conditions of laminar and turbulent flow, and then the permeate fluxes will be analyzed by the resistance-in-series model and the modified gel-polarization model to obtain equations for predicting permeate flux.

THEORY

Resistance-in-Series Model

In this model the permeate flux, J_v, is expressed as

$$J_v = \frac{\Delta P}{R_m + R_f + R_p} \tag{1}$$

where R_m is the intrinsic membrane resistance, and R_p and R_f are, respectively, the resistances due to the concentration polarization/gel layer and those due to other fouling phenomena such as solute adsorption. The viscosity of the permeate (essentially that of water due to the nearly complete rejection of the solute) has been included in those resistance terms. ΔP is the mean transmembrane pressure, defined as

$$\Delta P = \frac{p_i + p_o}{2} - p_p \tag{2}$$

where p_i and p_o are, respectively, the inlet and outlet pressure of the tubeside, and p_p is the permeate pressure of the shellside.

When pure water is ultrafiltrated with a fresh membrane module, neither R_p nor R_f exists, and Eq. (1) is reduced to

$$J_w = \Delta P/R_m \tag{3}$$

Therefore, the membrane resistance, R_m, is the slope of the straight line with $1/J_w$ as the ordinate and $1/\Delta P$ as the abscissa.

R_p will be proportional to the amount and the specific hydraulic resistance of the deposited layer on the membrane. When the applied pressure is increased, the thickness of the deposited layer grows, and R_p is a function of pressure:

$$R_p = \phi \Delta P \tag{4}$$

where ϕ is a function of feed concentration and feed velocity. Thus, Eq. (1) can be rewritten as

$$J_v = \frac{\Delta P}{R_m + R_f + \phi \Delta P} \tag{5}$$

in which R_m, R_f, and ϕ can be determined with the use of experimental data. It is noted from Eq. (5) that when ΔP is low, J_v is primarily controlled by $(R_m + R_f)$, and when ΔP is large, J_v will approach the value of $1/\phi$.

Modified Gel-Polarization Model

Ultrafiltration is a pressure-driven process whose permeate flux is proportional to the transmembrane pressure for small applied pressures, and which approaches a limiting flux, $J_{v,lim}$, when the transmembrane pressure becomes sufficiently large. Accordingly, the permeate flux may be defined as (19)

$$J_v = \frac{\Delta P}{R + \Delta P / J_{v,lim}} \tag{6}$$

Combination of Eqs. (5) and (6) results in the following relationships:

$$R = R_m + R_f \tag{7}$$

and

$$J_{v,lim} = 1/\phi \tag{8}$$

According to the gel-polarization model, the limiting flux is expressed as

$$J_{v,lim} = k \ln \frac{c_g}{c_b} \tag{9}$$

where c_b and c_g are solute concentrations in the bulk fluid and in the gel layer, respectively, and k is the average mass-transfer coefficient.

For a laminar flow system, the Leveque equation (2) may be used to evaluate the mass-transfer coefficient:

$$k = 1.62\left(\frac{u_b D^2}{2 r_m L}\right)^{1/3} \tag{10}$$

where u_b is the bulk velocity of the fluid, D is the solute diffusion coefficient in the bulk solution, and r_m and L are the radius and the length of the tubular membrane, respectively.

In a turbulent flow system, the mass-transfer coefficient may be evaluated by the Dittus–Boelter equation (2):

$$k = 0.023 \frac{u_b^{0.8} D^{0.67}}{(2r_m)^{0.2}(\mu/\rho)^{0.47}} \tag{11}$$

where μ and ρ are the viscosity and density of the bulk fluid, respectively. For macromolecular solutions, the theoretical permeate fluxes predicted by the gel-polarization model with the mass transfer coefficient obtained from Eq. (10) or Eq. (11) are 15–30% below the experimental data (2).

Since the permeate flux J_v is low compared with the flow velocity u in the ultrafiltration process, the bulk concentration, viscosity, density, and velocity may be assumed to be the same as those of inlet values, i.e., $c_b \approx c_i$, $\mu \approx \mu_i$, $\rho \approx \rho_i$, and $u_b \approx u_i$. Further, the diffusivity coefficient in the boundary layer is hard to estimate precisely because the concentration within it is uncertain. For convenience and precision, the mass-transfer coefficient in Eq. (9) is evaluated by Eq. (10) or Eq. (11) with the use of inlet solution properties and then multiplied by a modified factor F. So Eq. (9) becomes

$$J_{v,lim} = k_i F \ln \frac{c_g}{c_i} \tag{12}$$

where

$$k_i = 1.62\left(\frac{u_i D_i^2}{2r_m L}\right)^{1/3} \tag{13}$$

for the laminar flow system and

$$k_i = 0.023 \frac{u_i^{0.8} D_i^{0.67}}{(2r_m)^{0.2}(\mu_i/\rho_i)^{0.47}} \tag{14}$$

for the turbulent flow system.

EXPERIMENTAL METHOD

Apparatus and Materials

The flow diagram of an ultrafiltration apparatus is shown in Fig. 1. The feed solution was circulated by a high-pressure pump with a variable speed motor (L-07553-20, Cole-Parmer Co.), and the feed flow rate was measured with a flowmeter (IR-OPFLOW 502-111, Hedland Co.). The gauge pressure was measured with a pressure transmitter (Model 891.14.425, Wika Co.).

A tubular membrane (Carbsep M2, Tech-Sep, $2r_m = 6 \times 10^{-3}$ m, $L = 0.4$ m, and MWCO = 15,000 Da) module was employed. It was made of ZrO_2-TiO_2/carbon, and the total effective membrane area was 7.54×10^{-3} m^2.

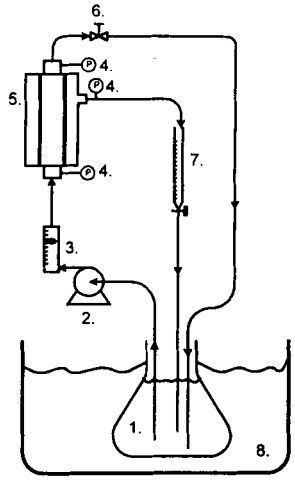

1. feed tank
2. pump
3. flow meter
4. pressure gauge
5. membrane module
6. pressure control valve
7. collector
8. thermostat

FIG. 1 Flow diagram of crossflow ultrafiltration apparatus.

The solute tested was dextran T500 (Pharmacia Co., M_n = 519,000, M_w/M_n = 2.2). It was more than 99% retained by the membranes used. The solvent was distilled water.

Experimental Conditions and Procedure

The experimental conditions were as follows. The feed concentrations, c_i, were 2.0, 4.0, 8.0, and 12.0 g/L; the feed velocities, u_i, were 0.15, 0.20, 0.25, 0.30, 0.50, 0.70, and 0.90 m/s; and the inlet gauge pressures, p_i, were 32.0, 58.8, 78.4, 98.01, 117.6, 156.8, and 196.0 kPa. The feed solution temperature was kept at 30°C in all experiments by a thermostat, and the gauge pressure in the permeate side was zero. Both the permeate and retentate were recycled back to the feed tank during a run to keep the feed concentration constant.

The experimental procedure was as follows. First, a fresh membrane module was used to determine the intrinsic resistance of the membrane. Permeate fluxes for pure water were measured under various transmembrane pressures. Then the permeate fluxes of the tested solutions, J_v, were measured under all operating conditions at steady state.

After each solution run the membrane module was cleaned by a combination of high circulation and backflushing with NaOH solution, HNO_3 solution, and pure water. The cleaning procedure was repeated until the original water flux had been restored.

RESULTS AND DISCUSSION

Table 1 is the experimental permeate flux data of pure water, J_w, and Table 2 is the experimental data of solution permeate flux, J_v, for the flows in both laminar (Re < 2100) and turbulent regions (Re > 2100). The Reynolds number, Re, is defined by $\rho_i u_i/(2r_m)/\mu_i$, in which the density of the feed solution, ρ_i, is related to that of water, and the viscosity of the feed solution, μ_i, is calculated approximately by

$$\mu_i = \mu_w \exp(0.037 c_i) \text{ Pa·s} \tag{15}$$

where the viscosity of water, μ_w, is taken as 0.89×10^{-3} Pa·s. For example, Re = 1870 for the case of c_i = 2.0 g/L and u_i = 0.30 m/s, and Re = 2150 for the case of c_i = 12.0 g/L and u_i = 0.50 m/s.

Determination of R_m

The membrane resistance, R_m, of the tubular membrane module employed can be determined from Eq. (3) coupled with the use of data in Table 1 by the method of least squares. It was found that

$$R_m = 4.59 \times 10^9 \text{ Pa·m}^2\text{·s·m}^{-3} \tag{16}$$

TABLE 1
Experimental Flux Data of Pure Water

$\Delta P \times 10^{-5}$ Pa	$J_w \times 10^6$ m^3·m^{-2}·s^{-1}
0.50	10.88
0.70	15.61
0.89	19.61
1.09	23.66
1.28	27.71
1.48	31.34
1.68	36.30
1.88	39.98

TABLE 2
Experimental Flux of Dextran T500 Solution

(a) Laminar Flow System, Re < 2100

	u_i = 0.15 m·s^{-1}		u_i = 0.20 m·s^{-1}		u_i = 0.25 m·s^{-1}		u_i = 0.30 m·s^{-1}	
c_i (g·L^{-1})	$\Delta P \times 10^{-5}$ Pa	$J_v \times 10^6$ m^3·m^{-2}·s^{-1}	$\Delta P \times 10^{-5}$ Pa	$J_v \times 10^6$ m^3·m^{-2}·s^{-1}	$\Delta P \times 10^{-5}$ Pa	$J_v \times 10^6$ m^3·m^{-2}·s^{-1}	$\Delta P \times 10^{-5}$ Pa	$J_v \times 10^6$ m^3·m^{-2}·s^{-1}
2.0	0.57	2.47	0.57	2.69	0.56	3.00	0.56	3.34
	0.77	2.64	0.76	2.89	0.76	3.24	0.76	3.67
	0.96	2.77	0.96	3.00	0.95	3.44	0.95	3.85
	1.16	2.85	1.15	3.14	1.15	3.55	1.15	4.05
	1.55	2.96	1.54	3.26	1.54	3.68	1.54	4.62
4.0	0.56	2.02	0.57	2.28	0.56	2.44	0.56	2.65
	0.76	2.16	0.76	2.45	0.76	2.64	0.76	2.87
	0.96	2.25	0.96	2.55	0.95	2.73	0.95	3.03
	1.15	2.32	1.15	2.65	1.15	2.83	1.15	3.15
	1.55	2.42	1.54	2.73	1.54	2.95	1.54	3.26
8.0	0.58	1.62	0.56	1.76	0.56	1.93	0.56	2.10
	0.76	1.72	0.76	1.86	0.76	2.06	0.76	2.26
	0.96	1.82	0.96	1.95	0.95	2.16	0.96	2.34
	1.15	1.86	1.15	2.02	1.15	2.22	1.15	2.42
	1.55	1.93	1.55	2.11	1.52	2.32	1.54	2.56
12.0	0.57	1.32	0.57	1.47	0.56	1.64	0.56	1.79
	0.76	1.39	0.76	1.55	0.76	1.76	0.75	1.92
	0.96	1.44	0.96	1.62	0.96	1.83	0.95	2.04
	1.15	1.50	1.15	1.67	1.15	1.89	1.15	2.07
	1.55	1.55	1.55	1.73	1.55	1.95	1.55	2.14

(b) Turbulent Flow System, Re > 2100

	u_i = 0.50 m·s^{-1}		u_i = 0.70 m·s^{-1}		u_i = 0.90 m·s^{-1}	
c_i (g·L^{-1})	$\Delta P \times 10^{-5}$ Pa	$J_v \times 10^6$ m^3·m^{-2}·s^{-1}	$\Delta P \times 10^{-5}$ Pa	$J_v \times 10^6$ m^3·m^{-2}·s^{-1}	$\Delta P \times 10^{-5}$ Pa	$J_v \times 10^6$ m^3·m^{-2}·s^{-1}
4.0	0.35	3.21	0.33	3.57	0.30	3.61
	0.54	4.16	0.53	4.85	0.49	5.30
	0.74	4.82	0.72	5.96	0.69	6.56
	1.13	5.48	1.11	6.88	1.08	8.02
	1.52	5.84	1.49	7.41	1.47	8.69
	1.91	6.08	1.88	7.95	1.86	9.41
8.0	0.35	1.91	0.31	1.96	0.30	2.11
	0.54	2.55	0.51	2.82	0.50	3.08
	0.74	3.15	0.70	3.51	0.69	3.92
	1.13	3.93	1.09	4.71	1.08	5.27
	1.52	4.25	1.48	5.32	1.47	6.17
	1.91	4.61	1.87	5.69	1.87	6.69
12.0	0.33	1.65	0.33	1.83	0.32	1.94
	0.53	2.22	0.53	2.60	0.51	2.80
	0.72	2.66	0.72	3.10	0.71	3.81
	1.12	3.19	1.12	3.78	1.09	4.91
	1.51	3.52	1.51	4.38	1.48	5.10
	1.90	3.84	1.90	4.74	1.88	5.62

Determination of R and $J_{v,lim}$

The experimental flux data can be correlated by Eq. (5) or Eq. (6) in the following form

$$\frac{1}{J_v} = \phi + \frac{(R_m + R_f)}{\Delta P} \tag{17}$$

or

$$\frac{1}{J_v} = \frac{1}{J_{v,lim}} + \frac{R}{\Delta P} \tag{18}$$

It was found from the experimental data listed in Table 2 that under a specified flow velocity u_i and feed concentration c_i, a straight line of $1/J_v$ vs $1/\Delta P$ can be constructed by the method of least squares. Therefore, the values of $1/J_{v,lim}$ (or ϕ) and R (or $R_m + R_f$) are the intercept on the ordinate and the slope of the least-squares lines, respectively. All the values determined from the experimental data are listed in Table 3, in which R_f is determined by the relation, $R - R_m$.

Analysis by Resistance-in-Series Model

The values of ϕ and R_f listed in Table 3 are functions of u_i and c_i. According to the methods employed in previous work (17), the correlation equations for ϕ and R_f can be found, so the permeate flux equations can be obtained. The correlated results are

$$\phi = 8.96 \times 10^4 \, u_i^{-0.49} c_i^{0.37} \tag{19}$$

$$R_f = 2.64 \times 10^8 \, u_i^{-0.63} c_i^{0.75} \tag{20}$$

$$J_v = \frac{\Delta P}{4.59 \times 10^9 + 2.64 \times 10^8 \, u_i^{-0.63} c_i^{0.75} + 8.96 \times 10^4 \, u_i^{-0.49} c_i^{0.37} \Delta P} \tag{21}$$

for the laminar flow region, and

$$\phi = 5.20 \times 10^4 \, u_i^{-0.99} e^{0.047 c_i} \tag{22}$$

$$R_f = 1.54 \times 10^8 \, u_i^{-0.25} c_i^{1.69} \tag{23}$$

$$J_v = \frac{\Delta P}{4.59 \times 10^9 + 1.54 \times 10^8 \, u_i^{-0.25} c_i^{1.69} + 5.20 \times 10^4 \, u_i^{-0.99} e^{0.047 c_i} \Delta P} \tag{24}$$

for the turbulent flow region. The difference in the concentration depen-

TABLE 3
Fitting Parameters for Experimental Flux Data[a]

c_i ($g \cdot L^{-1}$)	u_i ($m \cdot s^{-1}$)	$R \times 10^{-9}$ $m^2 \cdot Pa \cdot s \cdot m^{-3}$	$R_f \times 10^{-9}$ $m^2 \cdot Pa \cdot s \cdot m^{-3}$	$\phi \times 10^{-5}$ $s \cdot m^{-1}$	$J_{v,lim}/k_i$
2.0	0.15	6.00	1.41	2.99	9.63
	0.20	5.86	1.27	2.69	9.72
	0.25	5.53	0.94	2.35	10.34
	0.30	5.67	1.08	1.98	11.53
4.0	0.15	7.15	2.56	3.68	7.61
	0.20	6.52	1.93	3.23	7.88
	0.25	6.13	1.54	3.00	7.87
	0.30	6.29	1.70	2.65	8.41
	0.50	6.22	1.63	1.28	6.39
	0.70	6.20	1.61	0.90	6.96
	0.90	5.99	1.40	0.71	7.24
8.0	0.15	9.08	4.49	4.59	5.81
	0.20	8.28	3.69	4.24	5.71
	0.25	7.73	3.14	3.82	5.89
	0.30	7.34	2.75	3.48	6.09
	0.50	13.05	8.46	1.45	5.75
	0.70	12.59	8.00	1.04	6.15
	0.90	11.90	7.31	0.83	6.28
12.0	0.15	10.04	5.45	5.83	4.37
	0.20	9.22	4.63	5.20	4.44
	0.25	8.55	3.96	4.56	4.70
	0.30	8.06	3.47	4.12	4.90
	0.50	14.40	9.81	1.85	4.62
	0.70	13.40	8.81	1.39	4.69
	0.90	13.05	8.46	0.97	5.51

[a] $R_f = R - R_m$, $R_m = 4.59 \times 10^9$ $m^2 \cdot Pa \cdot s \cdot m^{-3}$.

dence terms in Eqs. (19) and (22) results from the use of correlated techniques on the experimental data for the least-squares error.

Analysis by Modified Gel-Polarization Model

Determination of c_g and F

According to Eq. (12), if a straight line of $J_{v,lim}/k_i$ vs ln c_i is constructed from the experimental data by the method of least squares, the values of c_g and F can be determined from the intersection on the concentration axis and the slope of this straight line, respectively.

The diffusion coefficient for a dextran T500 solution of concentration c_i can be estimated by the following equation (20):

$$D_i \times 10^{11} = 1.20 + 2.61 \times 10^{-2} c_i - 4.17 \times 10^{-5} c_i^2 + 2.13 \times 10^{-8} c_i^3 \ \mathrm{m^2 \cdot s^{-1}} \quad (25)$$

The experimental values of $J_{v,lim}/k_i$ were calculated by using the data in Table 3 as well as Eqs. (13)–(15) and (25). The results are also presented in Table 3. The values of c_g and F for this ultrafiltration system in both laminar flow and turbulent flow were determined as shown in Fig. 2. The results are $c_g = 55.8$ g/L and $F = 3.02$.

Permeate Flux Equation

The equation of limited permeate flux was thus obtained when c_g and F in Eq. (12) were replaced by 55.8 and 3.02, respectively. Thus

$$J_{v,lim} = 3.02 k_i \ln \frac{55.8}{c_i} \quad (26)$$

where k_i is obtained for the laminar flow system by Eq. (13) and for the turbulent flow system by Eq. (14).

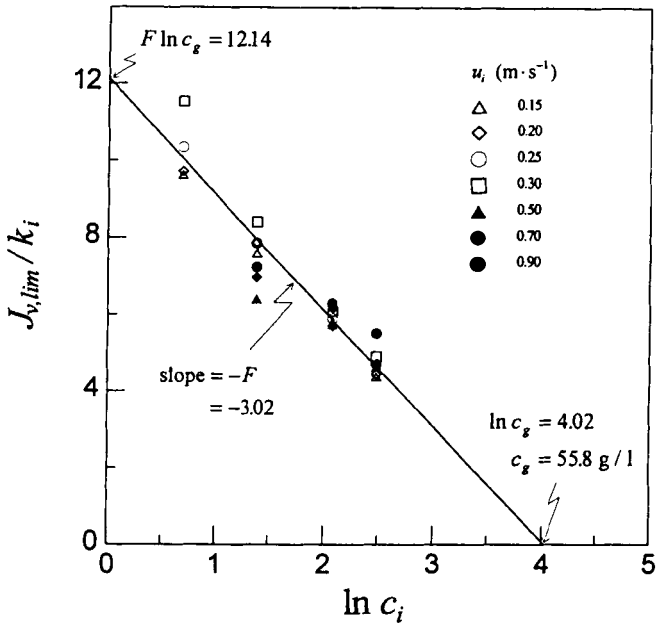

FIG. 2 Determination of c_g and F.

After obtaining the equation of limited permeate flux, the permeate flux for the laminar flow system or the turbulent flow system may be predicted by this model with the use of Eq. (6) and the corresponding resistance term R ($= R_m + R_f$) obtained in previous sections.

Resistance Analyses

The Fouling/Adsorption Resistance

Equations (20) and (23) are the correlation equations for the fouling/adsorption resistance R_f of this ultrafiltration system in laminar flow and turbulent flow respectively. Because these equations were rigidly obtained by the use of the least-squares technique on the experimental data, the mechanism of fouling is difficult to observe among these equations. However, it has been proved that the fouling/adsorption resistance depends on the concentration and the stagnant time of solute at the membrane surface. These concentration and stagnant time should vary with crossflow velocity and feed concentration, and thus the resistance R_f is dependent on crossflow velocity and feed concentration as shown in Eq. (20) or Eq. (23). Further, since a difference exists in the flow patterns of laminar flow and turbulent flow, the concentrations and the stagnant times of solute at the membrane surface are not the same, and this results in different forms of the correlation equations for R_p as shown by Eqs. (20) and (23), respectively.

The Concentration Polarization/Gel Layer Resistance

The concentration polarization/gel resistance R_p is known to be a function of the crossflow velocity on the membrane surface. In conventional treatment by the gel-polarization model (Eq. 9), the mass transfer coefficient in the concentration boundary layer is evaluated by using Eq. (10) or Eq. (11) with the inlet solution properties, but the theoretical flux predicted by this model is lower than the experimental data (2). This lower estimation of the limiting flux indicates that there is a higher power dependence of flux on the flow velocity than is suggested by Eq. (10) or Eq. (11).

In analysis by the resistance-in-series model, the resistance R_p decreases with flow velocity with the exponents 0.49 (Eq. 19) and 0.99 (Eq. 22) for the system in laminar flow and in turbulent flow, respectively. In another respect, the limiting flux will increase with crossflow velocity with the exponents 0.49 and 0.99 for laminar and turbulent systems, respectively, and these two values are greater than the values suggested by the gel-polarization model which are 0.33 (Eq. 10) and 0.8 (Eq. 11) for laminar and turbulent flows, respectively. Therefore, there is a higher

power dependence of flux on flow velocity than is indicated by Eq. (10) or Eq. (11).

In analysis by the modified gel-polarization model, the resistance R_p is represented by the mass transfer coefficient and a modified factor, where the mass transfer coefficient is linked to the diffusion coefficient and crossflow velocity. The modified factor F is introduced to modify the variousness of diffusion coefficient in the polarization layer and improve the precision of flux prediction. In our analysis the modified factor was found to be 3.02 for both laminar and turbulent flow systems.

Comparison of Theoretical Results with Experimental Data

For the laminar flow system, the theoretical permeate fluxes, calculated both from the resistance-in-series model (Eq. 21) and the modified gel-polarization model (Eq. 6), as well as the experimental data shown in Table 2 for c_i = 12.0 g/L, are plotted in Fig. 3 for comparison. Similarly, the theoretical values of the permeate flux (calculated by Eqs. 24 and 6) and the experimental data for the turbulent flow system with c_i = 12.0

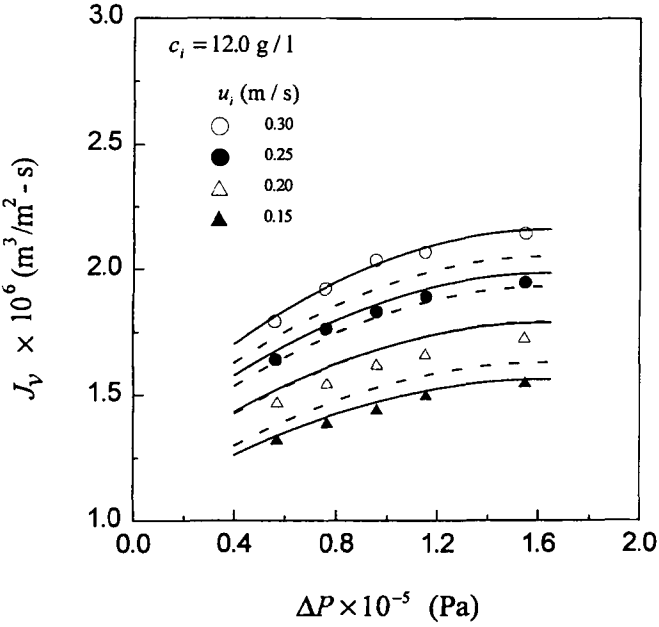

FIG. 3 Comparison of theoretical results with experimental data for laminar flow system: c_i = 12.0 g/L, solid lines calculated by resistance-in-series model, and dashed lines calculated by modified gel-polarization model.

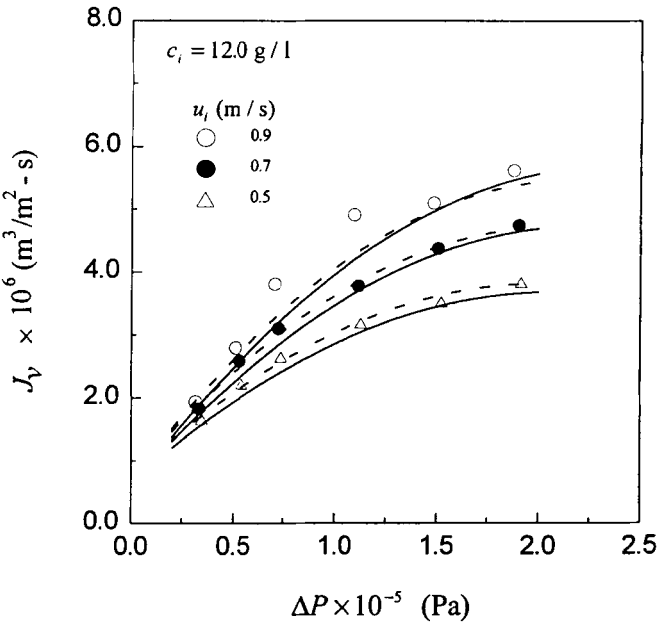

FIG. 4 Comparison of theoretical results with experimental data for turbulent flow system: c_i = 12.0 g/L, solid lines calculated by resistance-in-series model, and dashed lines calculated by modified gel-polarization model.

g/L are plotted in Fig. 4. It is seen from these figures that the resistance-in-series model (Eqs. 21 and 24) correlates the experimental data very well because the correlation equations are fitted by the same data. It is believed that these equations are also suitable for predicting flux in other operating conditions. It is seen that the fluxes predicted by the modified gel-polarization model (Eq. 6) also agree well with the experimental data.

As indicated by these comparisons, flux analysis by the resistance-in-series model or by the modified gel-polarization model is suitable not only for the laminar flow system but also for the turbulent flow system. Treatments by the modified gel-polarization model are easier to perform and the results possess more physical meaning than do those obtained by the resistance-in-series model.

CONCLUSIONS

The ultrafiltrated flux data of dextran T500 solutions in a tubular membrane module with membrane materials of ZrO_2-TiO_2/carbon have been

analyzed by the resistance-in-series model and the modified gel-polarization model, respectively. These flux analyses have been expanded to turbulent flow system in this work. The relationships between the resistances and the operating parameters, such as transmembrane pressure, flow velocity, feed concentration, etc., have been obtained by analysis of the resistance-in-series model. In analysis by the modified gel-polarization model, the mass transfer coefficient was found to be correlated by multiplication by a modified factor. The permeate flux predicted from these models agrees well with the experimental data.

The fouling/adsorption resistance depends on the concentration and the stagnant time of solute at the membrane surface. Since the flow patterns are different in laminar and turbulent flows, the concentration and the stagnant time of solute at the membrane surface are not alike, resulting in different forms of the correlation equations for R_f.

The resistance due to the concentration polarization/gel layer decreases with an increase in the flow velocity. In this work the resistance R_p was found to decrease with flow velocity with exponents of 0.49 and 0.99 for laminar and turbulent flows, respectively. These values are greater than those suggested by the gel polarization model where they are 0.33 and 0.8 for laminar and turbulent flows, respectively.

SYMBOLS

c	solute concentration ($g \cdot L^{-1}$)
D	diffusion coefficient ($m^2 \cdot s^{-1}$)
J_v	permeate flux of solution ($m^3 \cdot m^{-2} \cdot s^{-1}$)
$J_{v,lim}$	limiting permeate flux of solution ($m^3 \cdot m^{-2} \cdot s^{-1}$)
J_w	permeate flux of pure water ($m^3 \cdot m^{-2} \cdot s^{-1}$)
k	mass transfer coefficient ($m \cdot s^{-1}$)
L	length of the tubular membrane (m)
p_i, p_o	inlet, outlet gauge pressure of the tubeside (Pa)
p_p	gauge pressure of the shellside (Pa)
ΔP	mean transmembrane pressure (Pa)
Re	Reynolds number, $\rho_i u_i (2r_m)/\mu_i$
R_f	resistance due to fouling phenomena ($m^2 \cdot Pa \cdot s \cdot m^{-3}$)
R_m	intrinsic resistance of membrane ($m^2 \cdot Pa \cdot s \cdot m^{-3}$)
R_p	resistance due to concentration polarization/gel layer ($m^2 \cdot Pa \cdot s \cdot m^{-3}$)
r_m	radius of the tubular membrane (m)
u	flow velocity ($m \cdot s^{-1}$)
ϕ	parameter of concentration polarization defined in Eq. (4) ($s \cdot m^{-1}$)

μ viscosity of solution (Pa·s)
μ_w viscosity of water (Pa·s)
ρ density of solution ($kg \cdot m^{-3}$)

Subscript

i inlet of tubeside

ACKNOWLEDGMENT

The authors express their thanks to the National Science Council for financial aid.

REFERENCES

1. W. F. Blatt, A. Dravid, A. S. Michael, and L. Nelsen, "Solute Polarization and Cake Formation in Membrane Ultrafiltration: Causes, Consequences, and Control Techniques," in *Membrane Science and Technology* (J. E. Flinn, Ed.), Plenum Press, New York, NY, 1970, pp. 47–97.
2. M. C. Porter, "Concentration Polarization with Membrane Ultrafiltration," *Ind. Eng. Chem., Prod. Res. Dev., 11*, 234 (1972).
3. R. B. Grieves, D. Bhattacharyya, W. G. Schomp, and J. L. Bewley, "Membrane Ultrafiltration of a Nonionic Surfactant," *AIChE J.*, 19, 766 (1973).
4. J. J. S. Shen and R. F. Probstein, "On the Prediction of Limiting Flux in Laminar Ultrafiltration of Macromolecular Solutions," *Ind. Eng. Chem. Fundam., 16*, 459 (1977).
5. A. G. Fane, C. J. D. Fell, and A. G. Waters, "The Relationship between Membrane Surface Pore Characteristics and Flux for Ultrafiltration Membrane," *J. Membr. Sci., 9*, 245 (1981).
6. A. G. Fane, "Ultrafiltration of Suspensions," *Ibid., 20*, 249 (1984).
7. A. A. Kozinski and E. N. Lightfoot, "Protein Ultrafiltration: A General Example of Boundary Layer Filtration," *AIChE J., 18*, 1030 (1972).
8. J. G. Wijmans, S. Nakao, and C. A. Smolders, "Flux Limitation in Ultrafiltration: Osmotic Pressure Model and Gel Layer Model," *J. Membr. Sci., 20*, 115 (1984).
9. W. Leung and R. F. Probstein, "Low Polarization in Laminar Ultrafiltration of Macromolecular Solutions," *Ind. Eng. Chem. Fundam., 18*, 274 (1979).
10. S. Nakao and S. Kimura, "Models of Membrane Transport Phenomena and Their Applications for Ultrafiltration Data," *J. Chem. Eng. Jpn., 15*, 200 (1982).
11. C. Kleinstreuer and M. S. Paller, "Laminar Dilute Suspension Flows in Plate-and-Frame Ultrafiltration Units," *AIChE J., 29*, 529 (1983).
12. M. J. Clifton, N. Abidine, P. Aptel, and V. Sanchez, "Growth of the Polarization Layer in Ultrafiltration with Hollow-Fiber Membranes," *J. Membr. Sci., 21*, 233 (1984).
13. R. P. Ma, C. H. Gooding, and W. K. Alexander, "A Dynamic Model for Low-Pressure Hollow-Fiber Ultrafiltration," *AIChE J., 31*, 1728 (1985).
14. G. A. Denisov, "Theory of Concentration Polarization in Cross-Flow Ultrafiltration: Gel-Layer Model and Osmotic-Pressure Model," *J. Membr. Sci., 91*, 173 (1994).

15. B. H. Chiang and M. Cheryan, "Ultrafiltration of Skimmilk in Hollow Fibers," *J. Food Sci.*, *51*, 340 (1986).
16. H. Nabetani, M. Nakajima, A. Watanabe, S. Nakao, and S. Kimura, "Effects of Osmotic Pressure and Adsorption on Ultrafiltration of Ovalbumin," *AIChE J.*, *36*, 907 (1990).
17. H. M. Yeh and T. W. Cheng, "Resistance-in-Series for Membrane Ultrafiltration in Hollow Fibers of Tube-and-Shell Arrangement," *Sep. Sci. Technol.*, *28*(6), 1341 (1993).
18. A. Gomez-Gotor, P. Susial, A. Guerra, and B. Ibarra, "Experimental Data and Behavior of Starch/Water Solutions with an Ultrafiltration Module," *Ibid.*, *31*(2), 173 (1996).
19. H. M. Yeh, "Modified Gel-Polarization Model for Ultrafiltration in Hollow-Fiber Membrane Modules," *Ibid.*, *31*(2), 201 (1996).
20. J. G. Wijmans, S. Nakao, J. W. A. Van Den Berg, F. R. Troelstra, and C. A. Smolders, "Hydrodynamic Resistance of Concentration Polarization Boundary Layers in Ultrafiltration," *J. Membr. Sci.*, *22*, 117 (1985).

Received by editor August 29, 1996
Revision received March 1997